Analytical Chemistry Research 3 (2015) 20–25

Contents lists available at ScienceDirect

Analytical Chemistry Research

journal homepage: www.elsevier.com/locate/ancr

Unambiguous evaluation of the relative photolysis rates of nitro indolinyl protecting groups critical for brain network studies

Richard L. Comitz [a,b], Yannick P. Ouedraogo [a,c], Nasri Nesnas [a,*]

[a] Florida Institute of Technology, Department of Chemistry, Melbourne, FL 32901, USA
[b] Lieutenant Colonel US Army, Department of Chemistry and Life Science, United States Military Academy, West Point, NY 10996, USA
[c] Intel Corporation, Portland, OR, USA

ARTICLE INFO

Keywords:
Photolysis
Caged neurotransmitter
Photocage
Cage
Photoprotecting group
Nitro

ABSTRACT

Nitrated indolinyl photoprotecting groups are crucial tools extensively used in the study of neuronal signal transduction. Mononitrated photolabile protecting groups have been used effectively, however, recent advances in the introduction of a second nitro group have shown improvement in the photo efficiency of neurotransmitter (agonist) release, albeit, to varying extents, depending on the assessment methods employed. An unambiguous method is discussed based on Nuclear Magnetic Resonance (NMR), which is shown to be an effective technique in the relative overall rate comparison amongst varying nitrated protecting groups. Mononitrated and dinitrated photolabile protecting groups such as CDNI-Glu and MNI-Glu are used as an example to assess the relative value of adding a second nitro group in photoactive cage designs. Using this technique, it was shown that the second nitro group in CDNI systems enhances the overall relative rate of photocleavage by a factor of 5.8. This reported method can also be used to unambiguously determine relative rate of agonist photorelease.

1. Introduction

The mammalian brain contains a complex circuitry of neurons with numerous synaptic connections integrated with one another. For a thorough understanding of brain function and subsequently brain disorders, it is crucial to decode the neural circuitry with the resolution of a single synapse. Electrostimulation techniques lack such spatial resolution [1]. Neuroscience research endeavours have made recent use of neurological chemical tools known as caged neurotransmitters [1]. A caged neurotransmitter is a neurotransmitter, such as glutumate (Glu), attached to an inactivating molecular entity known as the cage. Photocleavable cages have gained popularity due to their ability to release the active neurotransmitter upon demand with a focused beam of photons of specific wavelengths. Newer technologies make use of two photon laser spectroscopy to enable superior penetrative light properties and a lower phototoxicity relative to the corresponding energy of a single photon in the UV region [2]. Photocleavable caged neurotransmitters enable a high degree of resolution leading to an ultimate spatio temporal control in the stimulation of a single synapse.

There has been a great deal of interest into the design of efficient cages for use in photolysis experiments [1]. It is inherently necessary to understand which properties can be altered to enhance photolysis. For instance, adding one nitro group to a mononitrated caged molecule renders this dinitrated compound more efficient [3]. However, it is not necessarily always straightforward to assess the photorelease efficiencies of these new molecular designs using UV–vis. Current methods use UV–vis as a technique to evaluate the role of having an additional nitro group on the nitroindolinyl ring. It is naturally the preferred means due to its rapid results and directness of measurement. However, as highlighted in the report by Timothy Dore and Hunter Wilson, there are inevitable challenges encountered when trying to assess the efficiency of mono and di-nitro molecules [4]. An unambiguous evaluation of the role of the additional nitro using sequential NMR measurements is presented herein. There is a need to introduce additional alternative methods to assess newly designed and synthesized molecules when they are not amenable to UV–vis interpretations. A recent report using 2D NMR to study reaction kinetics *in situ* was also highlighted [5]. In this communication, direct 1D ^{1}H NMR is used to gain reliable relative photorelease information with reproducible results.

The most common commercially available cage for a neurotransmitter is the 4-methoxy-7-nitroindolinyl cage. Remarkable advances in caged neurotransmitter design have been made

* Corresponding author at: Department of Chemistry, Florida Institute of Technology, 150 West University Boulevard, Melbourne, FL 32901, USA.
E-mail address: nesnas@fit.edu (N. Nesnas).

http://dx.doi.org/10.1016/j.ancr.2014.11.001
2214-1812/

independently by both Ellis-Davies [7] and Corrie [8] leading to cages that carry two nitro groups instead of one. One such example is the photochemical protecting group 4-methoxy-5,7-dinitroindolinyl (MDNI) which they both reported to show an improvement in quantum efficiency over its mononitrated analogue, (MNI) [7,8].

A related caging group, 4-carboxymethoxy-5,7-dinitroindolinyl (CDNI), was reported by Ellis-Davies [3] in 2007. It showed an improved solubility over MDNI due to the presence of a carboyxlate side chain in place of the methoxy group in MDNI. The presence of the additional nitro group on the cage (in MDNI and CDNI) improved the quantum efficiency of Glu release, as shown by UV–vis kinetic measurements. Using UV–vis kinetic measurement in the case of the mononitrated cage, MNI-Glu, was a direct and rapid technique to determine the kinetics of photorelease, resulting in a clear isosbestic point reflecting the clear presence of two distinct species, the starting caged compound and the spent cage. However, the additional nitro group, results in a UV–vis spectrum, which is somewhat less resolved with a less well-defined isosbestic point, rendering a more challenging kinetic evaluation of these improved cage designs. This could be due to several competing factors.

Although, ^{1}H NMR has been used for several years to gain kinetic information, it has not been employed in this way for photocaged molecules, except in showing the mere presence of the products. This research uses this NMR method as an alternative to make comparisons between the well-established MNI and MDNI cages, as evidence of our methodology, and for the additional benefit of using such technique to evaluate the relative rates of photorelease of our future cage designs. This is especially useful to researchers who may not have access to LASER photolysis equipment or Ultra High Performance Liquid Chromatography (UHPLC) apparatus.

2. Materials and methods

2.1. UV–vis studies

The rates of disappearance of the photochemical protective group were initially investigated using UV–vis studies, which, as mentioned above, have many advantages including low sample concentrations, rapid analysis, and ease of quantitation of results [9–12].

In all UV–vis studies the sample was dissolved in the appropriate solvent and serially diluted to the appropriate concentration. An aliquot was transferred into a UV cuvette which was then irradiated in a Rayonet photochemical reactor at 350 nm. UV–vis spectra were collected on a JASCO V-650 UV–vis spectrophotometer from 250 to 600 nm, and the predominant absorbance signals were fitted to a first-order decay or rise using Sigmaplot 11.

Commercially obtained MNI-Glu was dissolved in a water solution (pH = 7.39 with $NaHCO_3$) and serially diluted to a concentration of 0.074 mM. An aliquot was transferred into a clear UV cuvette which was then irradiated in a Rayonet® photoreactor at 350 nm [7,8,13]. MDNI-Glu and CDNI-Glu were synthesized from commercially available starting materials and UV experiments were run as above.

2.2. ^{1}H NMR studies

The general experimental set-up follows. A sample about 2 mM was transferred to a transparent quartz NMR tube which was then seated in a 125 mL Erlenmeyer flask and irradiated in the Rayonet photochemical reactor at 350 nm (75Wx16 UV lamps). After each irradiation period, a ^{1}H NMR spectrum was collected using a Bruker 400 MHz NMR. The NMR spectra were then calibrated for the solvent peak, and then a sample peak was chosen as an internal calibration. The data was fitted to global (common rate constant) and individual first-order decay, rise and second-order rise using the statistical software Sigmaplot 11®.

Commercially obtained MNI-Glu (0.33 mg in 0.500 mL D_2O, $[\ ]_0 = 2.04$ mM) was transferred to a transparent quartz NMR tube which was then seated in a 125 mL Erlenmeyer flask and irradiated in the Rayonet® photochemical reactor at 350 nm (75Wx16 UV lamps) for initially 20 s and subsequently 40 s intervals. After each irradiation period, a ^{1}H NMR spectrum was collected. The NMR spectra were then calibrated for the D_2O peak at 4.79 ppm, and the j+j' peaks integrated to 2.00, providing an internal calibration as the total concentration of caged Glu (j) and free Glu (j′) should always be 2 protons. Upon complete photolysis, the sample turned dark yellow from light yellowish beige. The data was fitted to global common rate constant and individual 1st order decay and rise to a maximum using the statistical software Sigmaplot 11®. MDNI-Glu and CDNI-Glu were synthesized from commercially available starting materials and ^{1}H NMR experiments were run as above.

3. Results

For the identification of free glutamic acid in the studied cages, Fig. 1 shows the UV–vis spectrum of glutamic acid on the same graph as the caged and uncaged MNI-Glu. This shows that the increasing absorption at 285 nm in this experiment and all of the caged glutamate experiments is due to the uncaged glutamate and the other absorbances are from either the cage molecule or remnant cage after photolysis.

For the commercially available MNI-Glu, results were reproducible and matched the published data for UV [6]. UV spectra were collected from 250 to 550 nm, and the absorbance at easily identifiable inflection points were fitted to a 1st order decay and rise to a maximum (Fig. 2).

The UV rates were more accurate (stronger R^2 correlation) for the rise at 403 nm than the decay at 332 nm. The 1st order rise to a maximum showed the highest rate constant (k) of 26.2×10^{-6} ms^{-1}. Overall, UV kinetics was fast but somewhat limited when assessing other cages or in providing mechanistic details.

Furthermore, MDNI-Glu was synthesized and the resultant UV spectrum was similar to those of Corrie et al. (Fig. 3) [8]. The UV rates showed a stronger R^2 correlation for the rise at 398 nm than the rise at 348–287 nm. The 1st order rise to a maximum showed

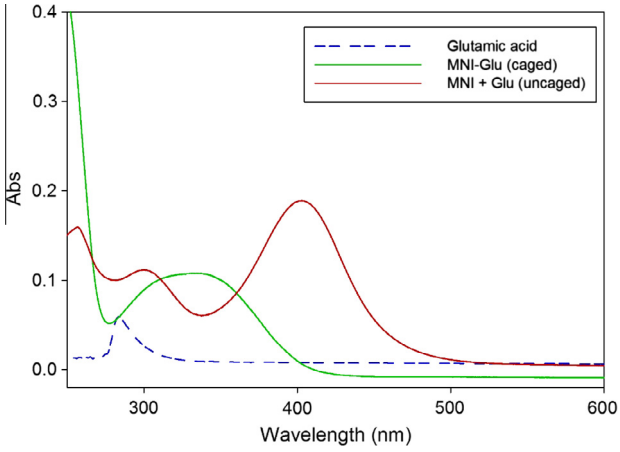

Fig. 1. Net UV–vis spectrum of glutamic acid, MNI-Glu (caged), and MNI + Glu (uncaged).

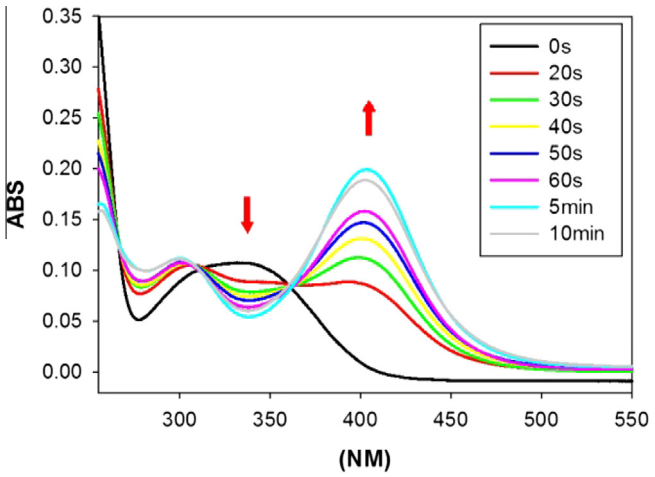

Fig. 2. UV–vis spectra for the progressive photolysis of MNI-Glu.

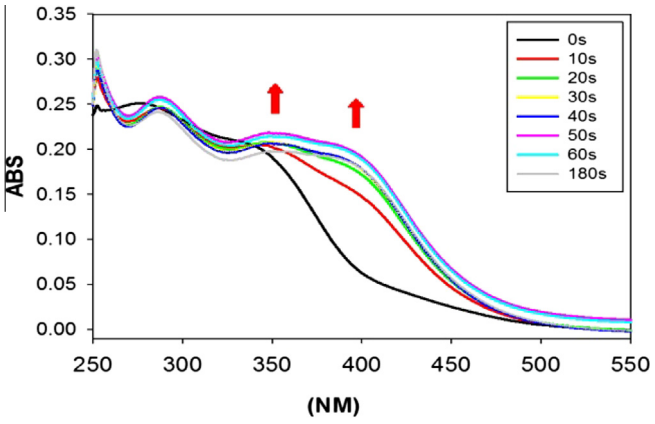

Fig. 3. UV–vis spectra for the progressive photolysis of MDNI-Glu.

the highest k value of 130×10^{-6} ms^{-1}. Upon the addition of the second nitro group, UV–vis spectra become more difficult to use in the determination of the rate of photolysis because of the absence of distinguishable inflection points.

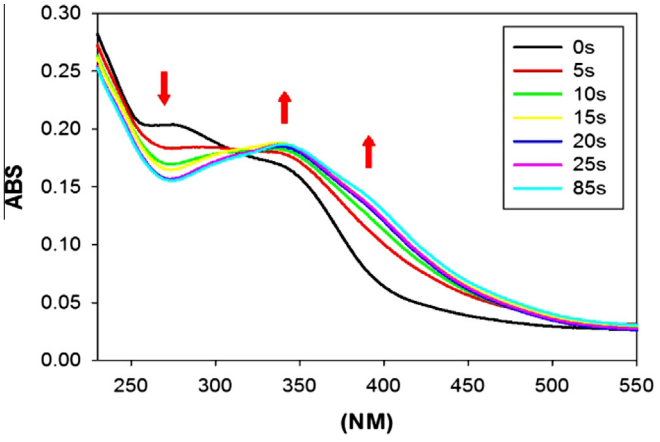

Fig. 4. UV–vis spectra for the progressive photolysis of CDNI-Glu.

CDNI-Glu was synthesized and the resultant UV–vis spectra was similar to those reported by Ellis-Davies in 2010 (Fig. 4) [14]. The 1st order rise to a maximum showed the highest k value of 172×10^{-6} ms^{-1}. As expected, CDNI-Glu had a similar UV profile to MDNI-Glu. The relative ratios for the rate constants (k) of photolysis were 1(MNI): 5 (MDNI): 6.4 (CDNI). These results support that the rate of photolysis is increased by adding a second nitro group.

Fig. 5 shows ^{1}H NMR photolysis of MNI-Glu, 2.04 mM, over time (from bottom to top) [15–17]. The initial protons (6, 5, 2, Me, i and j) disappear over time while new species (6′, 5′, 2′, Me′, i′, and j′) appear. These NMR peaks and integrals provide qualitative and quantitative information [10,18–25].

The decay data fitted a 1st order profile better as typically observed in the photokinetics of disappearing species. The individual rate constants (k) and observed rates (r) were very similar to the global fit values of 3.36×10^{-6} ms^{-1} for k and 6.87×10^{-6} ms^{-1} for r. These values were then used as a basis to compare other caged molecules.

The rates of appearance showed more interesting variations. The concerted (global fit) k value was about 1/3 less than that of the decay, and the error in k was also larger. The individual k values varied between 1.8 and 3.0×10^{-6} ms^{-1}. However, k values that were very similar strongly suggested that the species behaved similarly and may be undergoing the same transformations; thus, i' and j' likely remained attached with similar electronic environments resulting in a k of 2.3×10^{-6} ms^{-1}. Likewise, OMe′ and 6′ were combined as chemically behaving the same; although their lower k values suggested a rate limiting step and therefore an intermediate. H2′ and H3′ were of utmost interest because of their large and diverging k values; they most likely participated at different stages of the intermediate formation or conversion to the final product. The smaller k value of H2′ suggested that it was formed through a much slower process than H3′. Thus, ^{1}H NMR kinetics may, for the first time, explain the real dynamics of the involvement of H2 and H3 protons in the photolytic process that has been the source of speculation for decades [16].

The 2nd order rise to a maximum resulted in rate constants with lower values. These constants were further used with $[\text{MNI-Glu}]_0$ to determine the speciation concentration over time. The results showed a strong correlation with R^2 values close to unity. This correlation also provides evidence of intermediate species during the uncaging process.

Fig. 6 shows the ^{1}H NMR photolysis of MDNI-Glu, 2.9 mM. The experiment was performed as described above for MNI. The calculated rate constant was 13.6×10^{-6} ms^{-1} which is 4 times faster than MNI. When considering the observed rate, $r = 40 \times 10^{-6}$ ms^{-1}, MDNI is 5.8 times faster. These results are in line with the UV–vis photolysis experiments. They also support the hypothesis that a second nitro group improves the rate of photolysis.

Similar to MNI-Glu and MDNI-Glu (Figs. 5 and 6), CDNI-Glu, 3.9 mM, (Fig. 7) was uncaged in a Rayonet photoreactor at 350 nm, and the kinetics was studied by ^{1}H NMR. The determined rate constant for the 1st order kinetics was 10.6×10^{-6} ms^{-1}. Therefore, CDNI is 3.2 times faster than MNI cages under photolytic uncaging conditions [8,15,26]. The observed rate for CDNI was 37×10^{-6} ms^{-1}, which is 5.6 times faster. In both cases, CDNI is faster than MNI. As Ellis-Davies pointed out in his CDNI paper [3], a lower concentration can be used with dinitrated compounds, which would decrease the possibility of the caged molecule interfering with the neurological test being performed. Thus, a dinitrated cage can be administered at lower concentrations with improved performance over mononitrated compounds. Table 1 summarizes the relative kinetics of photolysis of MNI, MDNI and CDNI cages by ^{1}H NMR.

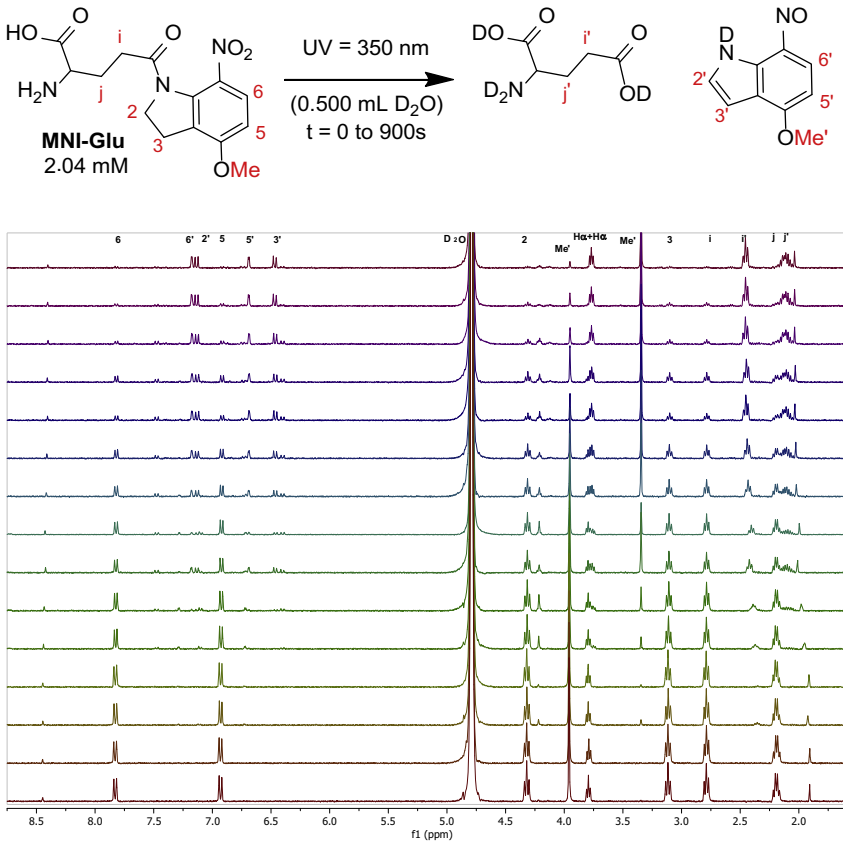

Fig. 5. ^{1}H NMR spectra for the progressive photolysis of MNI-Glu.

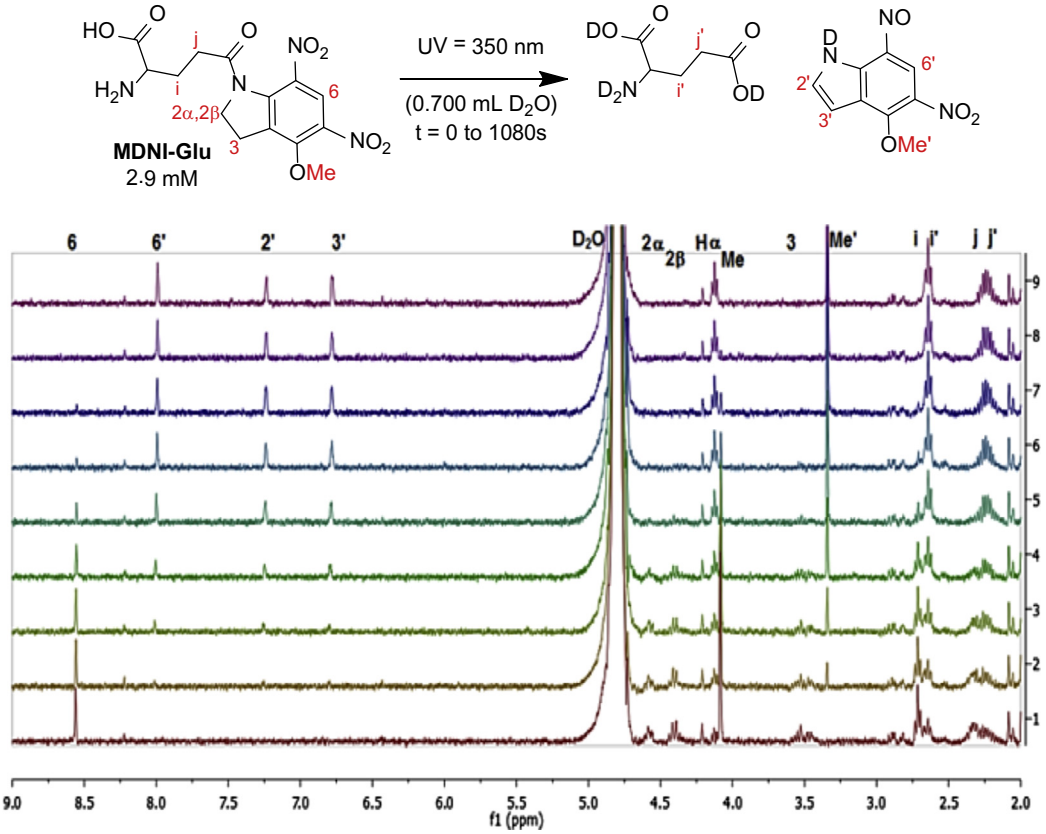

Fig. 6. ^{1}H NMR spectra for the progressive photolysis of MDNI-Glu.

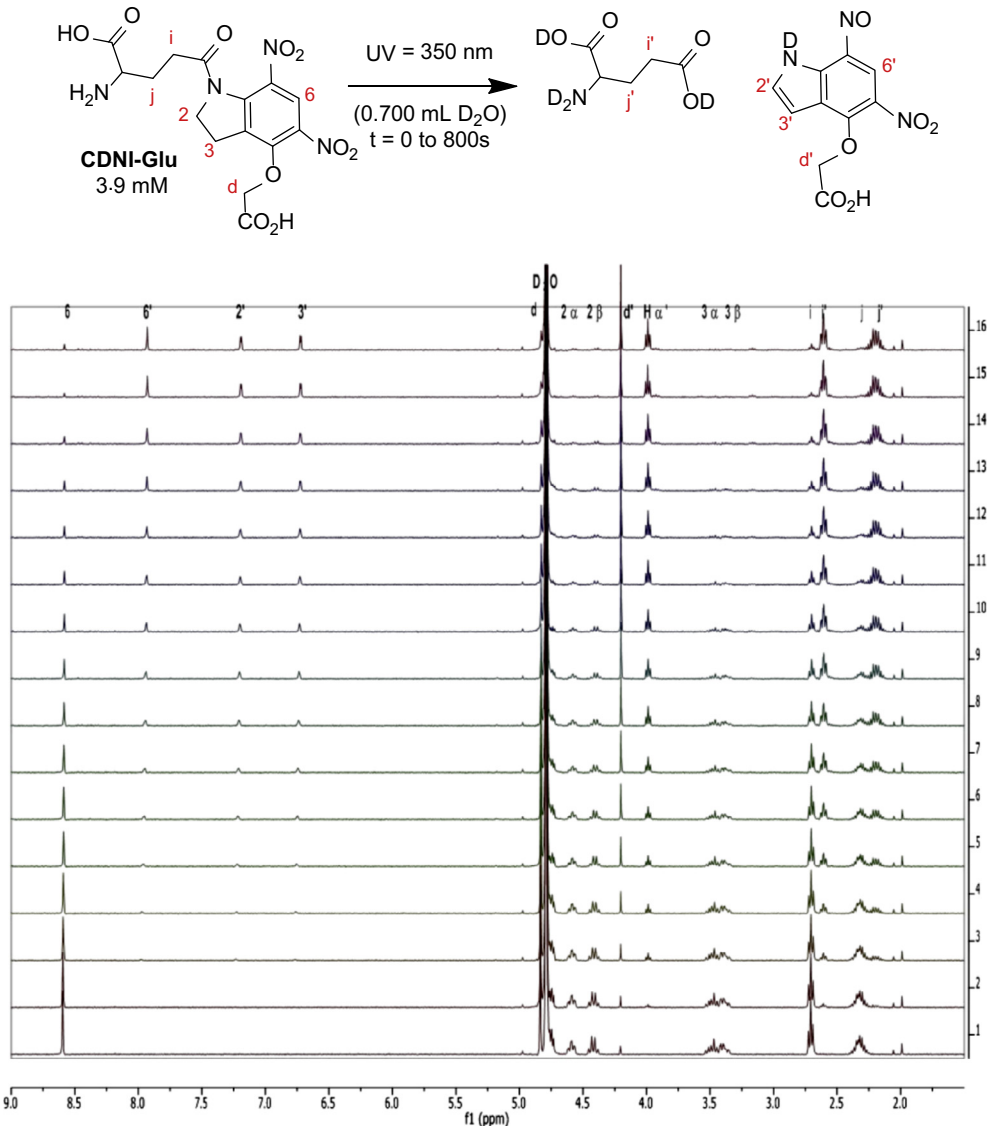

Fig. 7. ^{1}H NMR spectra for the progressive photolysis of CDNI-Glu.

Table 1
Summary of ^{1}H NMR photolysis results.

Cage	[ ] (mM)	k ($\times 10^{-3}$ s^{-1})	r ($\times 10^{-6}$ Ms^{-1})	k/k_{MNI}	r/r_{MNI}
MNI-Glu	2.0	3.36	6.9	N/A	
	1.9	3.36	6.2		
Avg	2.0	3.36	6.6		
MDNI-Glu	2.9	13.6	40	4.0	6.1
CDNI-Glu	–	10.8	–	3.2	–
	3.9	11.9	46	3.5	7.1
CDNI-GABA	3.5	11.3	39	3.4	6.0
	3.5	9.80	34	2.9	5.2
	3.3	9.02	29	2.7	4.4
Avg	3.6	10.6	37	3.1	5.7

4. Discussion

Although UV–vis generated rate constants for the photolysis of the caged Glu compounds are usually sufficient for mononitrated compounds, dinitrated compounds, such as MDNI and CDNI-Glu, show poorer fits (Table 2). Therefore, it appears that in this data, as well as those reported by established prior work [8], UV–vis in the case of cages with two nitro groups may suffer from a lack of clearly identifiable absorbance of individual species; that is, the observed peaks are a result of the sum of all species present. Moreover, these peaks may overlap, resulting in ambiguous inflection points. This may be due to the fact that the spent cage, as well as the caged dinitro molecule, contains a strongly withdrawing entity: the nitro group. In the case of MNI, the starting MNI-Glu contains one nitro which is lost to become a nitroso (not as electron withdrawing as the nitro), and the spent cage is therefore not as withdrawn, and hence will have a more distinct UV–vis spectrum.

To overcome the challenges encountered with UV–vis evaluation of dinitro systems, an alternative technique is introduced for such analyses taking advantage of direct monitoring of reaction progress with ^{1}H NMR, as a quantitative method for determining the efficiencies of photolysis. Advantages of this NMR technique, relative to the traditional UV–vis technique, include the ability to monitor the disappearance or appearance of individual protons as the photolysis progresses, the observation of any intermediates that may not only be easily observed by UV–vis, but also contribute

Table 2
Summary of UV–vis photolysis results.

UV Photolysis at 350 nm				
Rise: f = Abs_0 + Abs * (1 − exp(−k * x)); decay:			r = Obs. rate = $k^*[A]_0$	
	Wavelenght - Fit	Adj. R^2	k ($\times 10^{-3}$) s^{-1}	r ($\times 10^{-6}$ ms^{-1})
MNI-Glu UV (0.74 mM)	403 nm – rise(3)	1.000	26.2 ± 0.3	19.4 ± 0.2
ϕ Lit = 0.085	332 nm – decay(3)	0.988	25.0 ± 2.2	18.6 ± 1.6
	254 nm – decay(3)	0.998	26.7 ± 0.9	19.8 ± 0.7
MDNI-Glu UV (0.70 mM)	398 nm – rise(3)	1.000	130 ± 03	3.12 ± 0.08
ϕLit = 4.7	348 nm – rise(3)	0.974	142 ± 36	3.40 ± 0.86
CDNI-Glu UV (0.74 mM)	396 nm – rise (3)	0.983	168 ± 22	12.4 ± 1.6
ϕLit = 4.7	339 nm – rise(3)	0.943	172 ± 43	12.7 ± 3.2
	274 nm – decay(3)	0.991	114 ± 10	8.47 ± 0.77

to the challenge of interpretation of resulting spectra. Thus, using NMR, one can track the rate of change of each proton, giving more information on the mechanism of photolysis.

5. Conclusion

In conclusion, these experiments with mononitrated and dinitrated systems are in agreement with previous reports. The challenges faced in pinpointing the magnitude of the advantage of introducing an additional nitro group in cage design are circumvented using an alternative NMR method introduced in this work. The results showed at least a 3-fold rate improvement in all cases with the addition of a second nitro group.

^{1}H NMR was used as a method to accurately determine the rates of photolysis and to provide reproducible and easily interpretable data for the uncaging experiments, in general. Also, additional advantages of using this NMR technique in the potential to provide insight into the mechanism of photolytic cleavage of these photochemical protecting groups were highlighted. This method is relatively low cost and uses equipment that is considered standard in any synthetic lab and is, therefore, extensible to the future evaluation of the photolytic rates of newly designed and synthesized caged molecules.

Conflict of interest

The authors declared no conflict of interest.

Appendix A. Supplementary data

Supplementary data associated with this article can be found, in the online version, at http://dx.doi.org/10.1016/j.ancr.2014.11.001.

References

[1] G.C. Ellis-Davies, Caged compounds: photorelease technology for control of cellular chemistry and physiology, Nat. Methods 4 (2007) 619–628.
[2] G.C. Ellis-Davies, Two-photon microscopy for chemical neuroscience, ACS Chem. Neurosci. 2 (2011) 185–197.
[3] G.C.R. Ellis-Davies, M. Matsuzaki, M. Paukert, H. Kasai, D.E. Bergles, 4-Carboxymethoxy-5,7-dinitroindolinyl-glu: an improved caged glutamate for expeditious ultraviolet and two-photon photolysis in brain slices, J. Neurosci. 27 (2007) 6601–6604.
[4] T.M. Dore, H.C. Wilson, Chromophores for the delivery of bioactive molecules with two-photon excitation, in: J.J. Chambers, R.H. Kramer (Eds.), Photosensitive Molecules for Controlling Biological Function, Human Press, New York, 2011, pp. 57–92.
[5] Wu. Yuting, Carmine. D'Agostino, Daniel J. Holland, Lynn F. Gladden, *In situ* study of reaction kinetics using compressed sensing NMR, Chem. Commun. 50 (2014) 14137–14140.
[6] G. Papageorgiou, J.E.T. Corrie, Effects of aromatic substituents on the photocleavage of 1-acyl-7-nitroindolines, Tetrahedron 56 (2000) 8197–8205.
[7] O.D. Fedoryak, J.Y. Sul, P.G. Haydon, G.C. Ellis-Davies, Synthesis of a caged glutamate for efficient one- and two-photon photorelease on living cells, Chem. Commun. 29 (2005) 3664–3666.
[8] G. Papageorgiou, D. Ogden, G. Kelly, J.E.T. Corrie, Synthetic and photochemical studies of substituted 1-acyl-7-nitroindolines, Photochem. Photobiol. Sci. 4 (2005) 887–896.
[9] R.J. Silbey, R.A. Alberty, M.D. Bawendi, Physical Chemistry, Wiley, Hoboken, NJ, 2005.
[10] T. Ogoshi, D. Yamafuji, T. Aoki, T.A. Yamagishi, Photoreversible transformation between seconds and hours time-scales: threading of pillar [5] arene onto the azobenzene-end of a viologen derivative, J. Org. Chem. 76 (2011) 9497–9503.
[11] I. Zenz, H. Mayr, Electrophilicities of *trans*-β-nitrostyrenes, J. Org. Chem. 76 (2011) 9370–9378.
[12] D.A. Skoog, F.J. Holler, S.R. Crouch, Principles of Instrumental Analysis, Thomson Brooks/Cole, Belmont, CA, 2007.
[13] Y.H. Huang, S.R. Sinha, O.D. Fedoryak, G.C. Ellis-Davies, D.E. Bergles, Synthesis and characterization of 4-methoxy-7-nitroindolinyl-D-aspartate, a caged compound for selective activation of glutamate transporters and N-methyl-D-aspartate receptors in brain tissue, Biochemistry 44 (2005) 3316–3326.
[14] S. Kantevari, M. Matsuzaki, Y. Kanemoto, H. Kasai, G.C.R. Ellis-Davies, Two-color, two-photon uncaging of glutamate and GABA, Nat. Methods 7 (2010) 123–125.
[15] M. Goeldner, R. Givens, Phototriggers, photoswitches and caged biomolecule, in: Dynamic Studies in Biology, Wiley-VCH, Weinheim, 2005.
[16] J. Morrison, P. Wan, J.E. Corrie, G. Papageorgiou, Mechanisms of photorelease of carboxylic acids from 1-acyl-7-nitroindolines in solutions of varying water content, Photochem. Photobiol. Sci. 1 (2002) 960–969.
[17] H.J. Reich, W.H. Sikorski, A.W. Sanders, A.C. Jones, K.N. Plessel, Multinuclear NMR Study of the solution structure and reactivity of tris(trimethylsilyl)methyllithium and its iodine ate complex, J. Org. Chem. 74 (2009) 719–729.
[18] J.P. Smith, V. Hinson-Smith, Product review: high-resolution NMR gets even better, Anal. Chem. 73 (2001) 155A–158A.
[19] Y. Chen, J.L. Fulton, J.C. Linehan, T. Autrey, *In Situ* XAFS and NMR study of rhodium-catalyzed dehydrogenation of dimethylamine borane, J. Am. Chem. Soc. 127 (2005) 3254–3255.
[20] G. Horner, G.L. Hug, D. Pogocki, P. Filipiak, W. Bauer, A. Grohmann, A. Lammermann, T. Pedzinski, B. Marciniak, Head-to-tail interactions in tyrosine/benzophenone dyads in the ground and the excited state: NMR and laser flash photolysis studies, Chem. Eur. J. 14 (2008) 7913–7929.
[21] A.A. Marchione, P.J. Fagan, E.J. Till, R.L. Waterland, C. LaMarca, Estimation of atmospheric lifetimes of hydrofluorocarbons, hydrofluoroethers, and olefins by chlorine photolysis using gas-phase NMR spectroscopy, Anal. Chem. 80 (16) (2008) 6317–6322.
[22] W.J. Shaw, J.C. Linehan, N.K. Szymczak, D.J. Heldebrant, C. Yonker, D.M. Camaioni, R.T. Baker, T. Autrey, *In situ* multinuclear NMR spectroscopic studies of the thermal decomposition of ammonia borane in solution, Angew. Chem. Int. Ed. Engl. 47 (2008) 7493–7496.
[23] A.C. Stowe, W.J. Shaw, J.C. Linehan, B. Schmid, T. Autrey, *In situ* solid state ^{11}B MAS-NMR studies of the thermal decomposition of ammonia borane: mechanistic studies of the hydrogen release pathways from a solid state hydrogen storage material, Phys. Chem. Chem. Phys. 9 (2007) 1831–1836.
[24] A.J. Wand, S.W. Englander, Protein complexes studied by NMR spectroscopy, Curr. Opin. Biotechnol. 7 (1996) 403–408.
[25] J.C. Linehan, S.L. Wallen, C.R. Yonker, T.E. Bitterwolf, J.T. Bays, *In Situ* NMR Observations of the photolysis of cymantrene and methylcymantrene in supercritical fluids: a new technique using high-pressure NMR, J. Am. Chem. Soc. 119 (42) (1997) 10170–10177.
[26] M. Matsuzaki, G.C.R. Ellis-Davies, T. Nemoto, Y. Miyashita, M. Iino, H. Kasai, Dendritic spine geometry is critical for AMPA receptor expression in hippocampal CA1 pyramidal neurons, Nat. Neurosci. 4 (2001) 1086–1092.